Bull. Southern California Acad. Sci.
116(3), 2017, pp. 153–161

Geometric Morphometric Differentiation of Two Western USA Lizards (Phrynosomatidae: Squamata): *Uta stansburiana* and *Urosaurus ornatus*, with Implications for Fossil Identification

Julie E. Rej[1] and Jim I. Mead[2]

[1]*Department of Geosciences, East Tennessee State University, Box 70357, Johnson City, TN 37614, rejj01@etsu.edu*
[2]*The Mammoth Site, PO Box 692, Hot Springs, SD 57747*

Abstract.—Squamate fossil identification has been challenging due to the incomplete understanding and sometimes complete lack of osteological research of extant species. Here we compared the maxilla of two similar species of phrynosomatids: *Uta stansburiana* (Common Side-blotched Lizard) and *Urosaurus ornatus* (Ornate Tree Lizard). Through landmark-based geometric morphometric analyses, we determined which characters significantly separated the two species. A principle component analysis (PCA) and a stepwise discriminant function analysis (DFA) were conducted, in which we compared 15 landmarks between *U. stansburiana* and *U. ornatus*. Both the PCA and stepwise DFA showed separation between the two species. The stepwise DFA selected five of the 15 characters as statistically significant, three of which are considered apomorphies and show promise for fossil identification. The first character is in the ventral region of the posterior maxilla process; *U. ornatus* has a defined notch, whereas *U. stansburiana* does not. The second and third characters are in the anterior portion of the maxilla, which is curved dorsally in *U. stansburiana*, whereas *U. ornatus* shows no curving. The results of this study are used to identify fossil *Uta* vs *Urosaurus*, but more analyses need to be conducted on other phrynosomatid species for comprehensive identification.

Identification of fossil squamate reptiles (lizards and snakes) is typically a challenge due to the lack of comprehensive osteological collections of extant taxa. As a result, identification of isolated cranial elements is usually based on modern distributions of extant taxa, which leads to circular reasoning (Bell et al. 2009; Bell and Mead 2014). Additionally, the osteological apomorphies and patterns of variation at the species and genus level are unknown in most living taxa, making accurate identification often questionable. What is known is aptly presented, for example, in Lundelius (1957), Conrad (2008), Bhullar (2011), and Gauthier et al. (2012). Without proper identification of these organisms, more complex questions involving extinction, speciation, and geographic distribution cannot be adequately addressed.

Here we analyze the maxilla of two closely-related species of the Phrynosomatidae from western North America: *Uta stansburiana* (Common Side-blotched Lizard) and *Urosaurus ornatus* (Ornate Tree Lizard). These two species are typically considered indistinguishable from one another based on jaw (dentary and maxilla) and dental characteristics (Norell 1989). This is a problem because the majority of Neogene-age squamate fossils identified tend to be dentary and maxillary bones often due to collecting biases (Bell and Mead 2014). In the study here, we use geometric morphometric analyses on one bone, the maxilla, to find statistically significant characteristics that can be used to distinguish *U. stansburiana* from *U. ornatus*.

Uta stansburiana is one of the most abundant lizards found today in arid and semi-arid regions of western North America (Stebbins 2003). Living *U. stansburiana* are easily identified by the presence of a dark blotch on their side near the forelimb. They are predominately terrestrial and are found around rocks and low-ground bushes. The present range for *U. stansburiana* is from central Washington to the tip of Baja California, north Sinaloa and north Zacatecas Mexico, along the Pacific coast to west Colorado and west Texas, and many islands off of Baja and southern California. Fossil *U. stansburiana* are known from a variety of locations across Arizona: Brass Cap Point, Desert Almond, Vulture Cave, and Welton Hills (Mead 2005). They are considered a common species in the region during the Holocene and Late Pleistocene (Rancholabrean Land Mammal Age). Holocene-age fossils are also known from Howell's Ridge Cave in southern New Mexico (Van Devender and Worthington 1977; Harris 1993).

Urosaurus ornatus is a climbing lizard and is typically found on rocks and trees (Stebbins 2003). Their habitat ranges from the desert to the lower edge of spruce/fir zones. Living *U. ornatus* are distinguished by the large scales on their back, which are interrupted along the mid-line by small scales. The present range of *U. ornatus* is from southwestern Wyoming to Nayarit and northern Coahuila, Mexico (including Triburón Island in the Gulf of California), along the lower Colorado River valley central Texas, and into California to the Chuckwalla Mountains. Fossil *U. ornatus* are known from two locations in Arizona: Deadman Cave and Picacho Peak (Mead et al. 1984; Van Devender et al. 1991). Although *U. ornatus* is common in the region today, their fossil record is inadequately understood. Fossil forms are also known from Howell's Ridge Cave and U-bar Cave in southern New Mexico (Van Devender and Worthington 1977; Harris 1993).

Through geometric morphometrics, we determine if there is a morphological difference in the maxilla bone of *U. stansburiana* and *U. ornatus*. We predict there will be clear separation between the two groups. Also, we hope to obtain a list of statistically significant characters, which can be used to identify fossil forms using the maxilla. We picked these two taxa because our sample size of their skeletons was robust enough to be statistically sufficient. Correct identification of the isolated fossil skeletal elements is a problem for several species of phrynosomatids (Norell 1989; Bell et al. 2009), thus, we hope that this study will be the first step towards comprehensive fossil identification.

Materials and Methods

All modern specimens were in the ETSU (East Tennessee State University) vertebrate-paleo collections at the time of this study. Only disarticulated specimens were used to ensure consistent orientation. To reduce skewed results, only adults were used. To determine ontogenetic age, we checked the snout-vent length (SVL) data provided on the information tag of each specimen. According to Stebbins (2003), an adult *U. ornatus* SVL is 38-57 mm, and an adult *U. stansburiana* SVL is 38-63 mm. *Urosaurus ornatus* specimens were collected from: Arizona (counties: Pima, Coconino, Yavapai, and Cochise), Colorado, and Canyonlands National Park, Utah. *Uta stansburiana* specimens were collected from: Arizona (counties: Yavapai and Yuma), Yucca exit off of I-40 in Arizona, Burnt Springs Canyon at mile 259.5 along the Colorado River, Hidden Cave in Falon Nevada, San Bernardino county California, and a few unknown locations in California.

The bone selected for this study was the maxilla because they are common in the fossil record. Each specimen was photographed in labial view using a camera microscope. In labial view, the maxilla connects to the: jugal, lacrimal, pre-frontal, nasal, and pre-maxilla (Fig. 1A). The articulation surfaces with these bones have distinct processes, which are perfect for landmark locations (Fig. 1B). We selected the right maxilla, but if the right maxilla was unavailable or damaged, we used the left and reversed the image. Specimen orientation was consistent; the

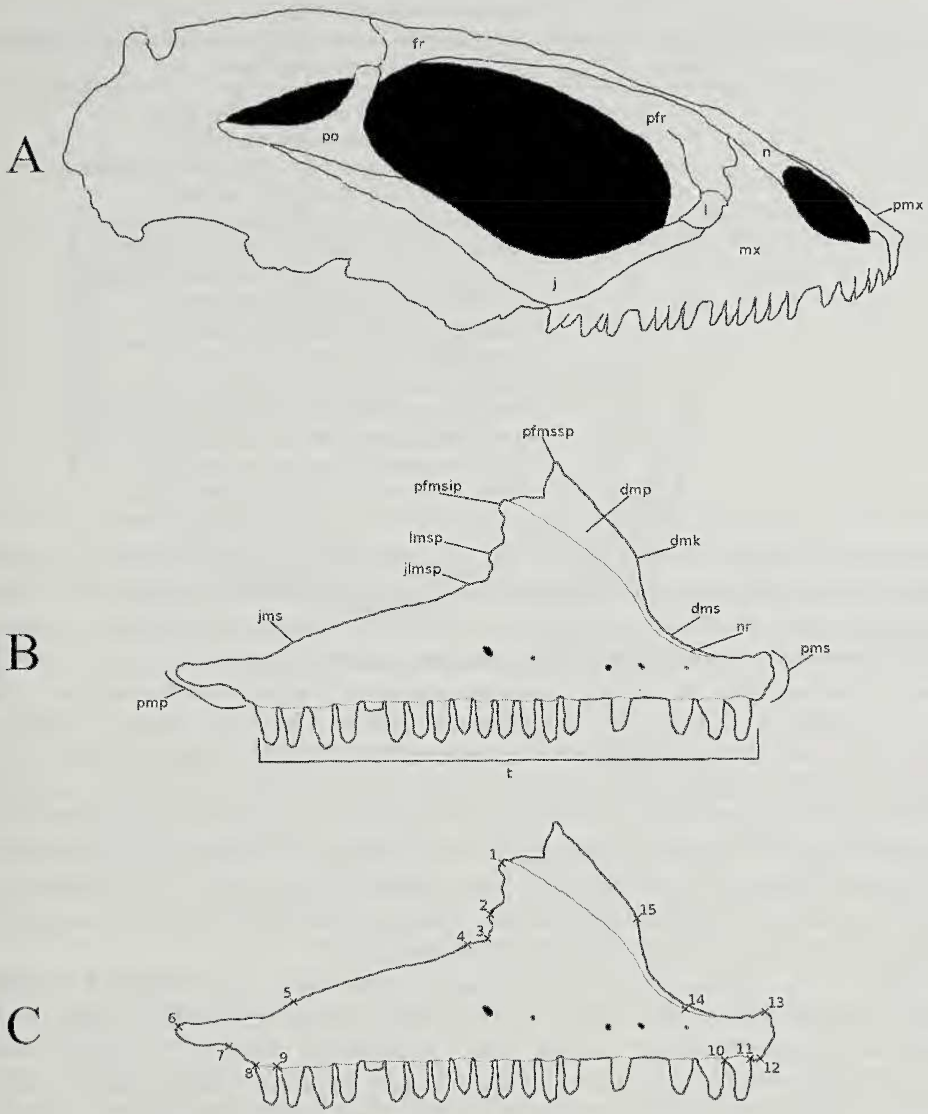

Fig. 1. A) Line drawing of *Urosaurus ornatus* skull showing the mx contact with: pmx, n, pfr, l, and j. B) Labeled diagram of *U. ornatus* maxilla in labial view. C) Location of landmarks on *U. ornatus* maxilla. See Methods and Materials for abbreviations.

premaxilla/maxilla suture, prefrontal/maxilla suture superior-process, and the palatine/maxilla suture (on lingual side) laid on an even piece of clay. Microscope photos were taken consistently at the same magnification. All photos were appended into a single thin-plate-spline (tps) file using tpsUtil (Rohlf 2016c). Next, a set of 15 2-dimensional landmarks were digitized onto 25 specimens of *U. stansburiana* and 24 specimens of *U. ornatus* using tpsDIG2 (Fig. 1C; Table 1; Rohlf 2016d). Landmark locations were predominantly on the perimeter of the maxilla and had to be present on every specimen in the analysis.

To align the data, we ran a single Procrustes fit using tpsSuper (Rohl 2016b). We used SPSS (IBM Corporation) to run the Principle Component Analysis (PCA) and the stepwise

Table 1. Description of landmark location.

Landmark	Location description
1	Tip of pfmsip: point of maximum curvature
2	Tip of lmsp: point of maximum curvature
3	Posterior base of dmp: point of maximum curvature
4	Tip of jlmsp: point of maximum curvature
5	Posterior ridge of jms: point of maximum curvature
6	Posterior tip of pmp: point of maximum curvature
7	Ventral notch of pmp: point of maximum curvature
8	Posterior base of the posterior most tooth
9	Anterior base of the posterior most tooth
10	Posterior base of the anterior most tooth
11	Anterior base of the anterior most tooth
12	Ventral edge of pms: point of maximum curvature
13	Dorsal edge of pms: point of maximum curvature
14	Curve of nr: point of maximum curvature
15	Tip of dmk: point of maximum curvature

Discriminant Function Analysis (DFA). The PCA was conducted to see if there is any initial separation between *Uta stansburiana* and *Urosaurus ornatus*. In addition, a stepwise DFA, with a significance level of 0.05, was also conducted on the data to examine separation and to determine which characters are significantly different between *U. stansburiana* and *U. ornatus*. Since this analysis was stepwise, the selected significant characters also showed little variation within a species which is important for determining apomorphies. Characters selected as significant by the stepwise DFA were examined in each specimen to determine consistency across both species. The PCA loading scores for each significant character on the first three components were reported to determine their contribution to the variance. Lastly, to test the mean differences in maxilla shape, a thin-plate-spline analysis was conducted to visualize species differences. To obtain a consensus for each species, we used tpsSuper (Rohl 2016b) to run a Procrustes fit for *U. ornatus* and *U. stansburiana* separately. Using tpsSpline (Rohl 2016a), we morphed the consensus of *U. ornatus* to the consensus of *U. stansburiana*.

Abbreviations. Abbreviations follow Hocknull (2000). **dmk**: dorsal maxilla kink, **dmp**: dorsal maxilla process, **dms**: dorsal maxilla process slope, **fr**: frontal, **j**: jugal, **jlmsp**: jugal/lacrimal/maxilla suture process, **jms**: jugal/maxilla suture, **l**: lacrimal, **lmsp**: lacrimal/maxilla suture process, **mx**: maxilla, **n**: nasal, **nr**: naris ridge, **pfmsip**: prefrontal/maxilla suture inferior-process, **pfmssp**: prefrontal/maxilla suture superior-process, **pfr**: prefrontal, **pmp**: posterior maxilla process, **pms**: premaxilla/maxilla suture, **pmx**: premaxilla, **po**: post-orbital, **t**: teeth.

Results

The PCA results are displayed in a 3-dimensional scatter plot where component score 1 is the X axis, component score 2 is the Y axis, and component score 3 is the Z axis (Fig. 2). The graph shows separation along the X axis (component 1) and along the Z axis (component 3). Separation is not clear along the Y axis (component 2); however, *U. stansburiana* data points have a wider distribution along the Y axis. Component 1 explains 24.47% of the variance with an eigen value of 7.34, component 2 explains 16.32% of the variance with an eigen value of 4.9, and component 3 explains 13.14% of the variance with an eigen value of 3.94.

Results from the stepwise DFA are displayed in a 2-dimensional bar-graph where the discriminant score 1 is on the X axis and frequency is on the Y-axis (Fig. 3). The graph shows

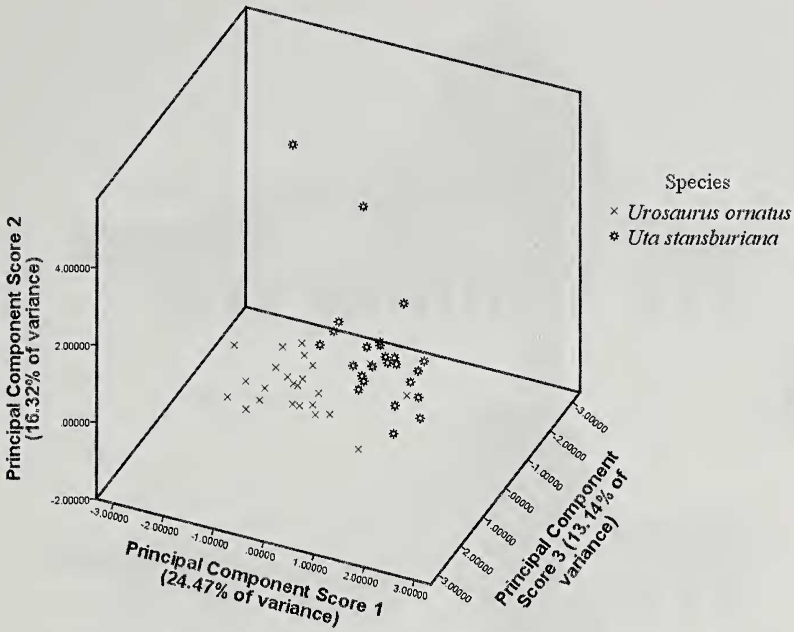

Fig. 2. Principle Component Analysis scatter plot.

clear separation (Fig. 3), with a significance value of 8.28E-19. The stepwise DFA selected five variables as statistically significant (Table 2). The PCA component loading scores and Wilk's Lambda values for each significant variable are listed in Table 2. Variables that consistently vary between *U. stansburiana* and *U. ornatus* are the ventral edge of the premaxilla/maxilla suture height (landmark 12, Y axis), posterior base of the anterior most tooth height (landmark 10, Y axis), ventral notch on the posterior maxilla process height (landmark 7, Y axis), posterior maxilla process tip height (landmark 6, Y axis), and lacrimal/maxilla suture process tip height (landmark 2, Y axis).

Component 1 has a high loading score for three of the significant variables: the ventral edge of the premaxilla/maxilla suture height, posterior base of the anterior most tooth height, and posterior maxilla process tip height. Component 3 loading score is high for the ventral notch on the posterior maxilla process height. The lacrimal/maxilla suture process tip height is the only significant variable to have a low loading score for all three components. Also, component 2 has a low loading score for all five significant characters.

Discussion

Both the PCA and the stepwise DFA show definitive separation (Fig. 2 and Fig. 3), which validates *U. ornatus* and *U. stansburiana* as morphologically separate species. PCA separation is observed along the X axis (component 1) and the Z axis (component 3). Of the five significant characters selected by the stepwise DFA, three have high loading scores on component 1 while one has a high loading score on component 3. Even though component 2 explains more of the variance then component 3, none of the significant characters had a high loading score on component 2. Additionally, separation is not clear along the Y axis (component 2) of the PCA; however, *Uta stansburiana* data points show more variation along the Y axis. This wide range amongst the *U. stansburiana* could be due to the species having more morphological variation

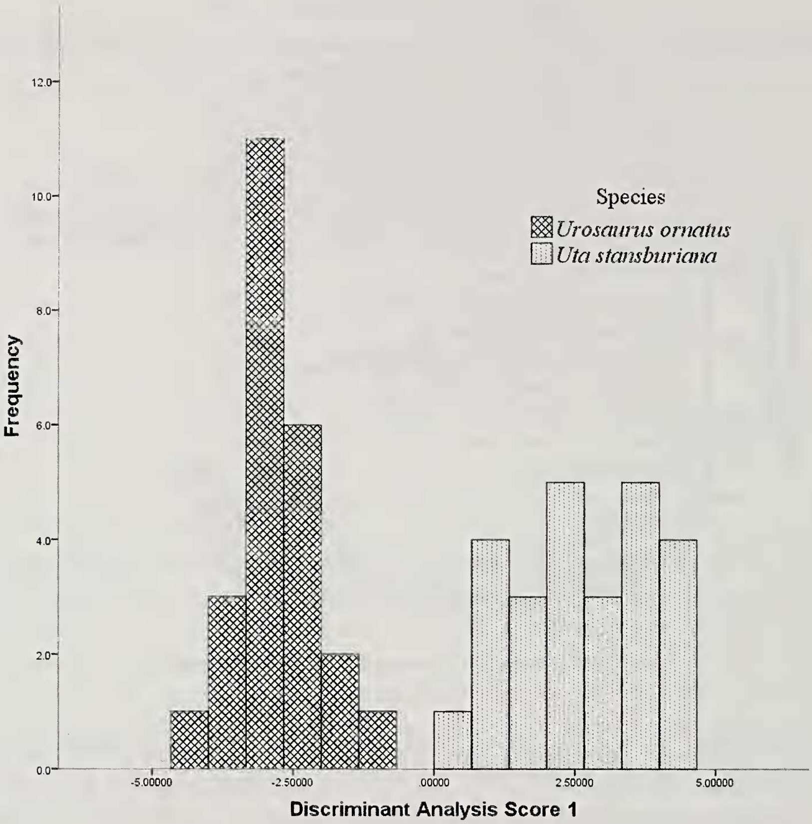

Fig. 3. Stepwise Discriminate function analysis bar graph.

compared to *U. ornatus*. Alternatively, the wide range could be due to abnormal specimens that are morphologically different from the rest due to pathologies, misidentification, or ontogenetic age. With a larger sample size collected from a variety of localities, the natural range of variation for each species would become clearer.

Based on the significant character's Wilk's Lambda values and observation of each specimen, the best three characters for differentiating *U. ornatus* from *U. stansburiana* are: 1) the ventral edge of the premaxilla/maxilla suture height, 2) the posterior base of the anterior most tooth height, and 3) the ventral notch on the posterior maxilla process height. These three statistically

Table 2. Variables kept by stepwise Discriminant function analysis.

Variables kept by stepwise DFA	Wilks' Lambda value	Significance score	Loading score from PCA for component 1	Loading score from PCA for component 2	Loading score from PCA for component 3
Y12	0.449	1.66E-10	0.841	−0.160	−0.359
Y10	0.219	2.71E-16	0.747	−0.478	0.230
Y7	0.133	5.41E-18	0.421	0.197	0.723
Y6	0.158	1.26E-18	0.693	0.248	−0.335
Y2	0.134	1.10E-18	−0.550	−0.262	−0.386

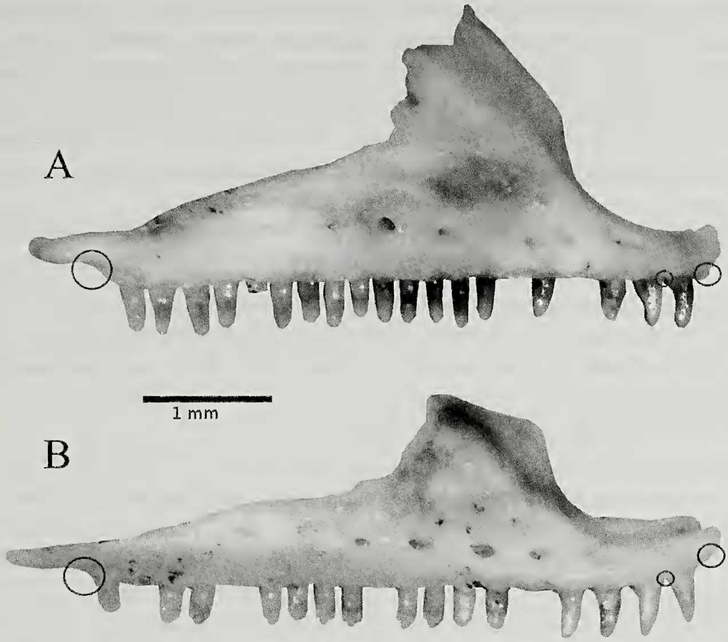

Fig. 4. Right maxilla in labial view: A) *Urosaurus ornatus* example specimen (JIM 0137) and B) *Uta stansburiana* example specimen (FB 1678). Statistically significant characters that were consistently observed in all specimens are circled.

significant characters had the highest Wilk's Lambda values (Table 2), and when examining each specimen of *U. ornatus* and *U. stansburiana*, these differences are very apparent. Fig. 4 shows an example specimen of each species, and the differences are circled. The pms is curved dorsally in *U. stansburiana*, and as a result, the anterior most tooth also curves dorsally. The pmp of *U. ornatus* has a distinct notch in the medial region. *U. stansburiana* has a similar notch in their pmp, but it occurs in the anterior region, caudally to the posterior most tooth. Furthermore, the thin-plate spline shows transformation in these characters when comparing the mean maxilla shape of *U. ornatus* and *U. stansburiana* (Fig. 5). These features are considered to be apomorphies and can be used to distinguish one species from the other.

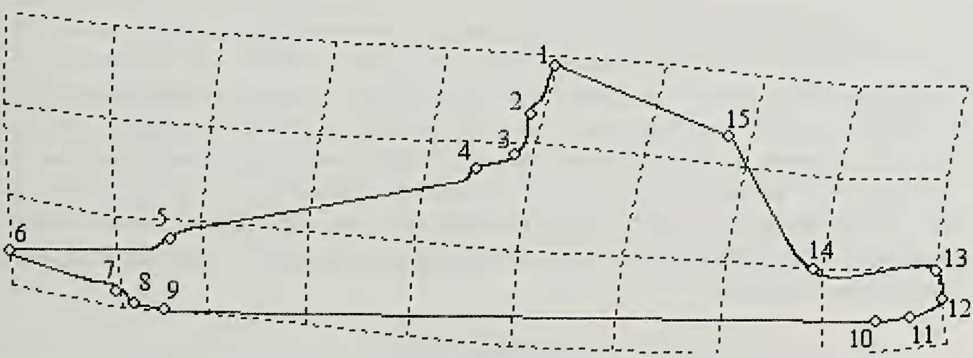

Fig. 5. Thin-plate splines showing the differences in mean maxilla shape. *Urosaurus ornatus* consensus has been morphed into the *Uta stansburiana* consensus.

Other characters selected as significant by the stepwise DFA were: 1) height of the posterior maxilla process tip, and 2) height of the lacrimal/maxilla suture process tip. These characters have lower Wilk's Lambda values, and noticeable differences between species are not apparent in every specimen observed. The pmp tip is curved dorsally in *U. ornatus*; however, this feature is not always consistent. Height of the lmsp varied greatly amongst all specimens, but the process appears to be slightly higher in *U. ornatus*. Additionally, height of the lmsp is the only significant character to have a low loading score for all eight components.

At first glance, *U. ornatus* might seem very different from *U. stansburiana*, for example, *U. stansburiana* does not have a visible pfmssp, while *U. ornatus* does (Fig. 4). It is important to note that this is not consistent and therefore is not a good character to use for identification. Also, *U. stansburiana* appears to have a clear differentiated nr from the dms, however this is also inconsistent amongst specimens. In *U. ornatus*, the lmsp is more pronounced and there exists a small process between the pfmsip and the lmsp, but these traits are also inconsistent, and therefore should not be used for identification.

There are a few characters that were not selected by the stepwise DFA that may seem useful because they are associated with the pms: the height of the ventral edge of the pms and the height of the anterior base of the anterior most tooth. Even if these characters showed a significant difference between species, they were possibly not selected as significant due to variation within a species, thereby failing the tolerance test. We conducted only a stepwise DFA because we wanted significant characters that were also consistent and showed little to no variation within a species. Characters that meet these criteria are considered apomorphies, and can be used to identify fossils.

The majority of the significant characters were along the Y axis, implying height differences in the maxilla, which could result in height differences in the face. Based on the observations of each specimen, *U. ornatus* has a taller face, whereas *U. stansburiana* has a short and squat face. The difference in face shape matches what is known about the biology of each lizard; *U. ornatus* is typically found on trees, while *U. stansburiana* is on the ground and hides under rocks (Stebbins 2003).

Conclusions

Despite past difficulties in identifying the two phrynosomatids *Urosaurus ornatus* and *Uta stansburiana*, there is a statistical difference when comparing the maxilla bone morphology. Three reliable characters can be used when distinguishing the maxilla of *U. ornatus* from *U. stansburiana*: 1) ventral edge of the premaxilla/maxilla suture height, 2) ventral notch on the posterior maxilla process height, and 3) posterior base of the anterior most tooth height. Since these character differences are observable in each specimen, they are considered apomorphies and can be used for fossil identification. Other less-reliable characters that have potential for identification are: 1) posterior maxilla process tip height, and 2) lacrimal/maxilla suture process tip height. These data are important for fossil identification because the maxilla is a common bone in the squamate fossil record and taxonomically significant characters are still unknown for several groups. Even though this study only examines two species, these results are encouraging and will hopefully result in similar studies using more taxa. It is important to continue morphometric analyses on different species and cranial elements for a more comprehensive guide to identify fossil squamates.

Literature Cited

Bell, C.J. and J.I. Mead. 2014. Not enough skeletons in the closet: collections-based anatomical research in an age of conservation conscience. Anat. Rec. 297:344–348.

———., J.A. Gauthier, and G.S. Bever. 2009. Covert biases, circularity, and apomorphies: a critical look at the North American Quaternary Herpetofauna Stability Hypothesis. Quatern. Int. 217:30–36.

Bhullar, B.A.S. 2011. The power and utility of morphological characters in systematics: a fully resolved phylogeny of *Xenosaurus* and its fossil relatives (Squamata: Anguimorpha). Bull. Mus. Comparat. Zool. 160:65–181.

Conrad, J.L. 2008. Phylogeny and systematics of Squamata (Reptilia) based on morphology. Bull. Am. Mus. Nat. Hist. 310:1–182.

Gauthier, J.A. 2012. Assembling the squamate tree of life: perspectives from the phenotype and the fossil record. B. Peabody Mus. Nat. Hist. 53:3–308.

Harris, A.H. 1993. Quaternary Vertebrates of New Mexico. New Mex. Mus. Nat. Hist. and Sci. Bull. 2:179–197.

Hocknull, S.A. 2002. Comparative maxillary and dentary morphology of the Australian dragon (Agamidae: Squamata): a framework for fossil identification. Mem. Queensland Mus. 48:125–145.

IBM Corporation. 2015. IBM SPSS statistics 21 core system user's guide. IBM Corporation, Armonk, 426 pp.

Lundelius, E.L. 1957. Skeletal adaptations in two species of *Sceloporus*. Evol. 11:65–83.

Mead, J.I. 2005. Late Pleistocene (Rancholabrean) amphibians and reptiles of Arizona. New Mex. Mus. Nat. Hist. and Sci. Bull. 29:137–152.

———., E.L. Roth, T.R. Van Devender, and D.W. Steadman. 1984. The late Wisconsinan vertebrate fauna from Deadman Cave, Southern Arizona. Trans. San Diego Soc. Nat. Hist. 20:247–276.

Norell, M.A. 1989. Late Cenozoic lizards of the Anza Borrego Desert, California. Contr. Sci. 414:1–31.

Stebbins, R.C. 2003. Side-blotched, brush, and tree lizards: genera *Uta* and *Urosaurus*. Pp. 295–297 in A field guide to western reptiles and amphibians, 3rd ed. Houghton Mifflin Co.

Rohlf, F.J. 2016a. tpsSplines (version 1.22). Department of Ecology and Evolution, University of New York at Stony Brook, Stony Brook, New York.

———. 2016b. tpsSuper (version 2.02). Department of Ecology and Evolution, University of New York at Stony Brook, Stony Brook, New York.

———. 2016c. tpsUtil (version 1.68). Department of Ecology and Evolution, University of New York at Stony Brook, Stony Brook, New York.

———. 2016d. tpsDIG2 (version 2.26). Department of Ecology and Evolution, University of New York at Stony Brook, Stony Brook, New York.

Van Devender, T.R. and R.D. Worthington. 1977. The herpetofauna of Howell's Ridge Cave and the paleoecology of the northwestern Chihuahuan Desert, in Wauer, R. H. and D. H. Riskind, eds. Trans. of the Symp. Bio. Res. Chihuahuan Des. Reg., US and Mexico. 3:85–106.

———., J.I. Mead, and A.M. Rea. 1991. Late Quaternary plants and vertebrates from Picacho Peak, Arizona. Southwest. Nat. 36:302–314.